Journal of Directed Energy, **3**, Summer 2010, 289–303

Exposure to Backscattered Laser Radiation

George Megaloudis and Edward Early*
TASC, Brooks City-Base, Texas 78235

and

Paul Kennedy
U.S. Air Force Research Laboratory, 711HPW/ RHDO, Brooks City-Base, Texas 78235

A laser beam propagating in the atmosphere undergoes scattering and absorption by atmospheric molecules and suspended particles. A portion of the scattered radiation is backscattered and propagates toward the location of the laser source. There is concern that the backscattered radiation produced by a high-energy laser may pose ocular or skin hazards to personnel in the vicinity of the laser source. To assess these hazards, equations are derived for the backscattered irradiance from both continuous-wave and pulsed lasers. The derivations are based on the definition of the atmospheric backscatter coefficient and the principles of beam propagation theory. The expression for the backscatter irradiance of a pulsed laser is shown to reduce to the LIDAR (LIght Detection And Ranging) equation under conditions that characterize typical remote sensing scenarios. The application of the derived equations to backscatter hazard assessments using the applicable ANSI standards for safe use of lasers is discussed.

KEYWORDS: Aerosols, Backscatter, Backscatter coefficient, Beam irradiance, Laser safety

Nomenclature

D_f	limiting aperture
$\mathrm{d}A$	area element in the x–y plane with its center at the origin
$\mathrm{d}V$	volume element in the space illuminated by the beam
$\mathrm{d}\sigma/\mathrm{d}\Omega$	differential light scattering cross section
$\mathrm{d}\Omega$	solid angle subtended by $\mathrm{d}A$ at the center of the volume element $\mathrm{d}V$
E_{CW}	continuous-wave (CW) beam irradiance
E_P	pulse irradiance
$E_{s,\mathrm{CW}}$	CW beam backscattered irradiance at the center of the laser aperture
$\tilde{E}_{s,\mathrm{CW}}(\rho)$	CW beam backscattered irradiance on the x–y plane at distance ρ from the center of the laser aperture
$E_{s,P}(t)$	backscattered pulse irradiance at the center of the laser aperture at time t
$\tilde{E}_{s,P}(\rho, t)$	backscattered pulse irradiance on the x–y plane at time t and distance ρ from the center of the laser aperture

Received March 5, 2010; revision received March 30, 2010.
*Corresponding author; e-mail: Edward.early@tasc.com.

$E_{s,L}$	irradiance of a LIDAR return pulse
f	beam focus distance
$h_p(z)$	altitude at the location on the slant propagation path that is at a distance z from the aperture center
M^2	beam quality
N_k	number of scatterers of type k per unit volume
Q	pulse energy
$Q_{s,P}$	effective energy of backscattered pulse
$\beta(z)$	backscatter coefficient at distance z from the aperture center along the propagation path
θ_b	beam $1/e$ half-angle divergence
λ	laser wavelength
μ	atmospheric extinction coefficient
ξ	normalized scalar field in the region $z \geq 0$
ρ	distance from the origin on the x–y plane
τ	pulse duration
$\tau_a(z)$	atmospheric attenuation from the aperture center to location z along the propagation path
Φ	CW beam power
$\Phi_{s,\mathrm{CW}}$	effective power of the backscattered radiation produced by a CW beam
$\Phi_{s,P(t)}$	backscattered pulse power passing through the limiting aperture at time t
ω_o	beam $1/e^2$ radius on the laser aperture

1. Introduction

Laser radiation propagating in the atmosphere is scattered and absorbed by molecules and suspended solid particles and liquid droplets. For high-energy lasers, the scattered radiation may pose ocular or skin hazards that must be quantified and evaluated prior to field tests or operational deployment. Of particular concern is the backscattered radiation, i.e., the radiation scattered in the direction opposite to the beam propagation direction, which may pose a hazard to personnel in the vicinity of the laser source.

Backscattered laser radiation is commonly used to measure atmospheric properties with a technique known as LIDAR (LIght Detection And Ranging). In a typical LIDAR application, laser pulses are transmitted vertically into the atmosphere and the backscattered signal is processed using the range resolution capabilities to estimate atmospheric properties as a function of altitude.[7] LIDAR systems have been used to measure such atmospheric properties as temperature, pressure, humidity, wind speed and direction, and aerosol (suspended particles and droplets) and trace gas concentrations.[3,4]

In LIDAR systems, the information of interest in the backscattered signal originates at long distances from the laser source, typically at least a kilometer. This information therefore arrives at the receiver some time after the outgoing pulse left the laser aperture. However, because backscattered laser radiation is produced as soon as the beam starts to exit the laser aperture, hazard assessments must quantify the backscattered irradiance starting at this time.

This paper provides a quantitative framework for hazard assessments of the backscattered laser radiation produced by both continuous-wave (CW) and pulsed beams. Models for CW and pulsed beams are derived and then applied to obtain approximate expressions

that quantify the backscattered irradiance at the plane of the laser aperture. The derived expressions for the backscattered irradiance of a pulsed beam are valid at all times after the pulse emerges from the laser aperture. Unlike the backscattered irradiance produced by a CW beam, which does not vary in time, the backscattered irradiance produced by a pulsed beam is shown to exhibit pulse-like characteristics.

A hazard assessment of the backscattered radiation from a CW or a pulsed laser beam requires the calculation of several parameters to implement the hazard evaluation procedures specified in the ANSI standard for safe use of lasers.[1] We discuss how the expressions for the backscattered irradiance derived in this paper are applied to calculate the required parameters.

2. Backscatter Coefficient

The backscatter coefficient is a measurable quantity that determines the backscattered irradiance. In this section, the backscatter coefficient is used to derive the differential backscattered irradiance at the center of the laser aperture. This irradiance is assumed to originate in a small-volume element illuminated by the beam. The total backscattered irradiance at the aperture center is then found by integrating the backscattered irradiance contributions of individual volume elements. In Sec. 3 we present beam models that, together with the expression for the differential irradiance derived in this section, are used to derive the total backscattered irradiance for both CW and pulsed beams.

The differential light scattering cross section, $d\sigma(\theta)/d\Omega$, of a single molecule or particle has units of square meters per steradian and relates the intensity of the light scattered at angle θ, $I(\theta)$ in units of watts per steradian to the incident irradiance E:

$$I(\theta) = E \cdot \frac{d\sigma(\theta)}{d\Omega}. \tag{1}$$

The scatter angle θ is measured counterclockwise from the propagation direction of the incident beam so that at $\theta = \pi(\theta = 0)$, the reflected intensity is in the direction opposite (parallel) to the beam propagation direction. In general, the differential scattering cross section of a single molecule or particle depends on the laser wavelength.

The backscatter coefficient, β, is defined by the expression

$$\beta = \sum_k \frac{d\sigma_k(\pi)}{d\Omega} \cdot N_k, \tag{2}$$

where N_k is the number of scatterers of type k per unit volume. The backscatter coefficient consists of contributions from all molecular and aerosol species that are present in the atmospheric volume illuminated by the beam. It follows from Eq. (2) that β has units of meters per steradian and, in general, depends on altitude, the prevailing atmospheric conditions, and the wavelength of the incident beam irradiance. We note that the molecular contribution to β is due primarily to the nitrogen and oxygen that make up 99% of the atmosphere's molecular constituents. The differential light scattering cross section of molecules is given by the Rayleigh formula.[5]

Figure 1 shows the coordinate system, the irradiance distribution of a hypothetical focused CW beam, and the differential volume and area elements used in the derivation of the differential backscattered irradiance. The laser aperture lies in the x–y plane, and the beam is assumed to propagate in the positive z direction along an arbitrary slant path through the atmosphere. This path begins at the coordinate system origin located at the center of

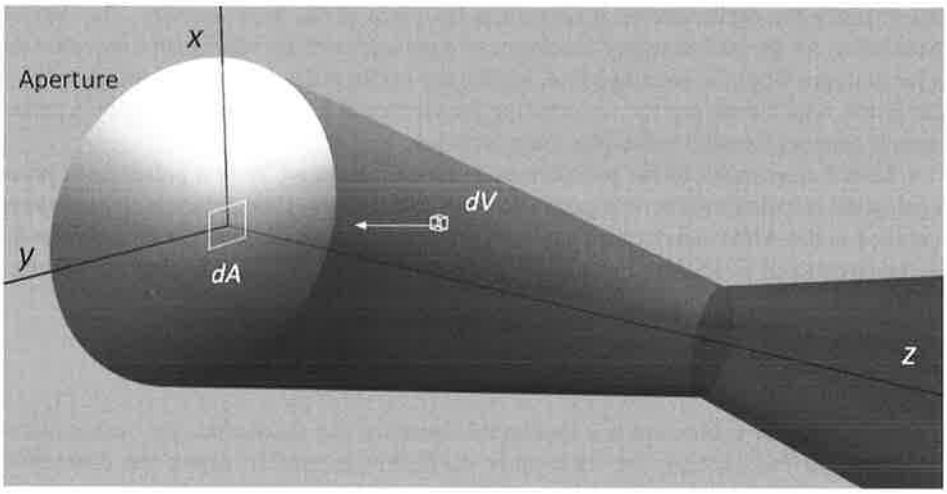

Fig. 1. Focused laser beam and the differential area and volume elements used to derive the backscattered irradiance.

the laser aperture, so that the z axis represents the distance from the origin along the path. Because both the backscatter and atmospheric extinction coefficients vary with altitude, they will also vary over the propagation path unless it is at constant altitude. To account for this variation with path distance, we introduce the path-dependent backscatter coefficient, $\beta(z)$, and atmospheric attenuation, $\tau_a(z)$. Both of these quantities may be obtained from backscatter and extinction measurements or model predictions at different altitudes. For example, let $\beta_m(h)$ represent the backscatter coefficient as a function of altitude h. Also, let the function $h_p(z)$ represent the altitude at the location on the slant path that is a distance z from the origin. Then, the path-dependent backscatter coefficient, $\beta(z)$, is given by $\beta_m[h_p(z)]$.

Consider the differential volume element $\mathrm{d}V$ shown in Fig. 1, defined as $\mathrm{d}V = \mathrm{d}x\mathrm{d}y\mathrm{d}z$ and centered at location (x, y, z). Using the definition of β and the beam irradiance incident on $\mathrm{d}V$, we find that the differential backscattered intensity, $\mathrm{d}I_s$, at the center of $\mathrm{d}V$ is given by

$$\mathrm{d}I_s = \beta(z) \cdot E(x, y, z) \cdot \tau_a(z) \cdot \mathrm{d}x\ \mathrm{d}y\ \mathrm{d}z, \tag{3}$$

where E is the unattenuated beam irradiance at $\mathrm{d}V$ and $\tau_a(z)$ accounts for atmospheric attenuation of the beam over the propagation path from the aperture to $\mathrm{d}V$. The solid angle $\mathrm{d}\Omega$, subtended by $\mathrm{d}A$ at the center of $\mathrm{d}V$, is

$$\mathrm{d}\Omega = \frac{z \cdot \mathrm{d}A}{(x^2 + y^2 + z^2)^{1.5}}. \tag{4}$$

Therefore, the backscattered power, $\mathrm{d}P$, passing through the area $\mathrm{d}A$ centered at the origin as shown in Fig. 1 is approximated by multiplying $\mathrm{d}I_s$ by $\mathrm{d}\Omega$ so that $\mathrm{d}P$ is given by

$$\mathrm{d}P = \beta(z) \cdot E(x, y, z) \cdot \frac{z \cdot \mathrm{d}A}{(x^2 + y^2 + z^2)^{1.5}} \cdot \tau_a^2(z) \cdot \mathrm{d}x\ \mathrm{d}y\ \mathrm{d}z. \tag{5}$$

In this expression, we have included an additional factor of $\tau_a(z)$ to account for atmospheric attenuation over the propagation path from dV back to the x–y plane. Dividing both sides of Eq. (5) by dA, we find that the differential backscattered irradiance at the origin is approximately given by

$$dE_s = \beta(z) \cdot E(x, y, z) \cdot \frac{z}{(x^2 + y^2 + z^2)^{1.5}} \cdot \tau_a^2(z) \cdot dx\, dy\, dz. \tag{6}$$

From Fig. 1, one can see that for volume elements near the x–y plane and relatively far from the z axis, the scatter angle θ to the origin will not be π radians as assumed in the derivation of Eq. (6). However, for the great majority of locations in the beam, the angle to the origin will be close to π radians because the extents of the beam along the x and y directions are small compared to its extent along the z direction. Moreover, for locations near the aperture plane and away from the z axis, the subtended solid angle is small so that their contribution to the irradiance at the origin will also be small.

Equation (6) shows that in order to assess the backscattered hazard associated with a specific high-energy laser test or deployment, one needs to know, or at least be able to estimate an upper bound for, the backscatter coefficient at the laser wavelength and the test or deployment location. This is complicated by the variability of aerosol species and their concentrations. Aerosols also vary in shape, with the majority having radii between 10^{-3} and 10 μm. Examples of aerosols include particles of dust, combustion by-products, fog, and possibly salt when droplets of sea spray evaporate. The scattering of light by spherical particles with arbitrary refractive index is described by the theory developed by Mie.[2] However, because aerosols are rarely spherical, the Mie theory is not always accurate.

Despite these challenges, models of aerosol light scattering properties have been developed based on measurements as well as theory. These models are representative of rural, urban, maritime, and tropospheric atmospheric conditions and are documented in Ref. 6. For each model, this document gives coefficients of extinction, scattering, and the angular scattering distribution as functions of wavelength and relative humidity. In the absence of site-specific backscatter measurements, the data may be used to estimate an upper bound for the backscatter coefficient at the location of interest.

3. Beam Irradiance Models

According to Eq. (6), calculation of the backscattered irradiance requires that we know the beam irradiance distribution in the scattering volume. In this section, we present parametric beam irradiance models that can be used to predict the backscattered irradiance from a CW or pulsed laser beam based on knowledge of beam parameters.

The unattenuated irradiance of a CW beam propagating parallel to the z axis, E_{CW}, is modeled as

$$E_{CW}(x, y, z) = \Phi \cdot |\xi(x, y, z)|^2, \tag{7}$$

where Φ is the beam power and $\xi(x, y, z)$ is the field in the space to the right of the x–y plane as shown in Fig. 1.

The pulsed beam model assumes that all pulses in the beam are identical and that they propagate along the positive z axis. With these assumptions the unattenuated irradiance, E_P, of a single propagating beam pulse is modeled as

$$E_P(x, y, z, t) = \frac{Q}{\tau} \cdot p\left(t - \frac{z}{c}\right) \cdot |\xi(x, y, z)|^2, \tag{8}$$

where Q is the pulse energy and τ is the pulse duration. The dimensionless function $p(t)$ is defined as

$$p(t) = 1 \quad \text{for } 0 \leq t \leq \tau,$$
$$p(t) = 0 \quad \text{otherwise.} \tag{9}$$

Therefore, at a given time t, the leading and trailing edges of the pulse are at locations $z = ct$ and $c(t - \tau)$, respectively. It follows that at $t = 0$ the leading edge of the pulse is at $z = 0$, i.e., in the plane of the exit aperture.

The field $\xi(x, y, z)$ is normalized so that for any value of z, its integral over the x–y plane is unity:

$$\int_{-\infty}^{\infty}\int_{-\infty}^{\infty} |\xi(x, y, z)|^2 \, dx \, dy = 1. \tag{10}$$

This condition ensures that the integral of E_{CW} over any plane perpendicular to the propagation direction equals the beam power. Equation (10) may also used to show that the integral of the single pulse irradiance given by Eq. (8) over the pulse duration and the plane perpendicular to the propagation direction equals the pulse energy, i.e.,

$$\int_{z/c}^{(z/c)+\tau} dt \int_{-\infty}^{\infty}\int_{-\infty}^{\infty} E_P(x, y, z, t) \, dx \, dy = Q. \tag{11}$$

In general, the beam spatial irradiance distribution will depend on the output from the laser and the optics used to transmit the beam. We use a beam irradiance model that has a Gaussian distribution, accounts for the effect of higher order modes that may be present, and describes unfocused as well as focused beams. In this model, $|\xi(x, y, z)|^2$ is given by

$$|\xi(x, y, z)|^2 = \frac{\exp\left[-(x^2 + y^2)/\omega^2(z)\right]}{\pi \cdot \omega^2(z)}, \tag{12}$$

where $\omega(z)$ is the $1/e$ beam radius and $\omega^2(z)$ is given by

$$\omega^2(z) = \frac{1}{2}\left[\left(\frac{\lambda}{\pi \cdot \omega_o} \cdot M^2\right)^2 z^2 + \omega_o^2 \cdot \left(1 - \frac{z}{f}\right)^2\right]. \tag{13}$$

Here, ω_o is the $1/e^2$ beam radius at the aperture. This model satisfies Eq. (10) and was derived with the assumption that the beam is not truncated by the aperture. In Eq. (13), λ is the laser wavelength, f is the focus distance, and M^2 is the beam quality. If the focus distance f goes to infinity in Eq. (13), the model describes an unfocused beam with its waist at the aperture and radius ω_o. In this case, the beam diverges with $1/e$ half-angle θ_b given by

$$\theta_b = \frac{1}{\sqrt{2}} \cdot \frac{\lambda}{\pi \cdot \omega_o} \cdot M^2, \tag{14}$$

which is seen to be M^2 times the $1/e$ half-angle divergence of the lowest-order Gaussian mode. In the literature, the divergence of this mode is often referred to as the "diffraction limit." For this reason, some authors refer to M^2 as the "times-diffraction-limit" parameter. The inclusion of beam quality in the model makes it possible to approximately account for the presence of higher order modes that have a higher beam divergence than the lowest-order Gaussian mode.

Note that the expressions for the backscattered irradiance derived in the next section are also valid for other irradiance models that are rotationally symmetric about the beam propagation axis. These models include, for example, top-hat beams and centrally obscured beams transmitted by on-axis telescopes. To derive the backscattered irradiance for any of these models, one has only to replace our model irradiance distribution [Eqs. (12) and (13)] with that of the new model in the integrals for the backscattered irradiance. The model irradiance distribution must be normalized in accordance with Eq. (10).

4. Backscattered Irradiance

4.1. CW beam

The total backscattered irradiance at the origin is found by summing the backscatter contributions from individual volume elements in the space occupied by the beam, or equivalently by integrating Eq. (6). Substituting the CW model irradiance given by Eq. (7) in Eq. (6) and integrating the result gives the total backscattered irradiance at the origin, $E_{s,\mathrm{CW}}$:

$$E_{s,\mathrm{CW}} = \Phi \cdot \int_0^\infty \int_{-\infty}^{\infty} \int_{-\infty}^{\infty} \cdot \frac{|\xi(x, y, z)|^2 \cdot \beta(z) \cdot \tau_a^2(z) \cdot z}{(x^2 + y^2 + z^2)^{1.5}} \cdot \mathrm{d}x\, \mathrm{d}y\, \mathrm{d}z. \tag{15}$$

This integral may be simplified by exploiting the rotational symmetry of $|\xi(x, y, z)|^2$ about the z axis. If we define $|\zeta(r, z)|^2$ as

$$|\zeta(r, z)|^2 = \frac{\exp\left[-r^2/\omega^2(z)\right]}{\pi \cdot \omega^2(z)} \tag{16}$$

and change the x and y variables of integration by the transformation

$$\begin{aligned} x &= r \cdot \cos\varphi, \\ y &= r \cdot \sin\varphi, \end{aligned} \tag{17}$$

we find that Eq. (15) may be written as

$$E_{s,\mathrm{CW}} = 2 \cdot \pi \cdot \Phi \cdot \int_0^\infty \int_0^\infty \frac{|\zeta(r, z)|^2 \cdot \beta(z) \cdot \tau_a^2(z) \cdot z}{(r^2 + z^2)^{1.5}} \cdot r \cdot \mathrm{d}r\, \mathrm{d}z. \tag{18}$$

The numerical evaluation of Eq. (18) is faster than that of Eq. (15).

Note that if the propagation path is one of constant altitude, h_0, then $\beta(z)$ in the integrand of Eq. (18) is a constant equal to the atmospheric backscatter coefficient at altitude h_0 and may therefore be taken out of the integral. Also, for this propagation path the two-way atmospheric attenuation in the integrand is given by $\exp[-2 \cdot \mu(h_0) \cdot z]$, where $\mu(h_0)$ is the atmospheric extinction coefficient at altitude h_0.

4.2. Pulsed beam

Consider the differential volume element $\mathrm{d}V$ shown in Fig. 1 and a single pulse that propagates in the positive z direction. The power backscattered at $\mathrm{d}V$ and time t into the solid angle $\mathrm{d}\Omega$ is denoted by $\mathrm{d}P_{\mathrm{d}V}(t)$ and is given by

$$\mathrm{d}P_{\mathrm{d}V}(t) = \beta(z) \cdot \frac{E_P(x, y, z, t) \cdot \mathrm{d}A \cdot z \cdot \tau_a(z)}{(x^2 + y^2 + z^2)^{1.5}}\, \mathrm{d}x\, \mathrm{d}y\, \mathrm{d}z, \tag{19}$$

where $E_P(x, y, z, t)$ is the pulse irradiance given by Eq. (8). The propagation from dV to the aperture plane introduces an additional time delay, so the backscattered power that passes through dA is

$$dP_{dA}(t) = \beta(z) \cdot \frac{E_P[x, y, z, t - (z/c)] \cdot dA \cdot z \cdot \tau_a^2(z)}{(x^2 + y^2 + z^2)^{1.5}} dx\, dy\, dz, \tag{20}$$

where we have included an additional factor of $\tau_a(z)$ to account for the attenuation over the path back to the x–y plane. If we make use of Eq. (8) in Eq. (20) and divide by dA, we find that the differential backscattered irradiance at the origin, $dE_{s,P}(t)$, is given by

$$dE_{s,P}(t) = \beta(z) \cdot \frac{Q}{\tau} \cdot p\left(t - \frac{2z}{c}\right) \cdot \frac{|\xi(x, y, z)|^2 \cdot z \cdot \tau_a^2(z)}{(x^2 + y^2 + z^2)^{1.5}} \cdot dx\, dy\, dz. \tag{21}$$

At a fixed time t, the factor $p[t - (2z/c)]$ is nonzero for values of z such that $0 \leq [t - (2z/c)] \leq \tau$ or equivalently if z lies between $[c(t - \tau)]/2$ and $ct/2$. In other words, the irradiance at the origin at an arbitrary time t, $dE_{s,P}(t)$, is determined when the leading and trailing edge of the pulse is located at $ct/2$ and $[c(t - \tau)]/2$, respectively. Therefore, the total backscattered irradiance at the origin at time t is obtained by integrating Eq. (21) to yield

$$E_{s,P}(t) = \frac{Q}{\tau} \cdot \int_{c(t-\tau)/2}^{ct/2} \int_{-\infty}^{\infty} \int_{-\infty}^{\infty} \frac{|\xi(x, y, z)|^2 \cdot \beta(z) \cdot \tau_a^2(z) \cdot z}{(x^2 + y^2 + z^2)^{1.5}} dx\, dy\, dz. \tag{22}$$

Equation (22) is valid when $t \geq \tau$. However, for times t such that $0 \leq t < \tau$, the pulse trailing edge location, $[c(t - \tau)]/2$, will be less than zero, which means that some portion of the pulse is in the region to the left of the exit aperture plane. This portion of the pulse does not contribute to the backscattered irradiance at the origin, so that for times t such that $0 \leq t < \tau$, the lower limit in the integral over z must be set to zero. Therefore, the backscattered irradiance at the origin from a single outgoing pulse is given for all times $t \geq 0$ by

$$E_{s,P}(t) = \frac{Q}{\tau} \cdot \int_{a}^{ct/2} \int_{-\infty}^{\infty} \int_{-\infty}^{\infty} \frac{|\xi(x, y, z)|^2 \cdot \beta(z) \cdot \tau_a^2(z) \cdot z}{(x^2 + y^2 + z^2)^{1.5}} dx\, dy\, dz, \tag{23}$$

where

$$a = 0 \quad \text{for } 0 \leq t < \tau,$$

$$a = \frac{c(t - \tau)}{2} \quad \text{for } t \geq \tau. \tag{24}$$

The integral in Eq. (23) may be simplified by making use of the rotational symmetry of $|\xi(x, y, z)|^2$ about the z axis. Changing variables of integration as in Eq. (17), we find that

$$E_{s,P}(t) = 2 \cdot \pi \cdot \frac{Q}{\tau} \cdot \int_{a}^{ct/2} \int_{0}^{\infty} \frac{|\zeta(r, z)|^2 \cdot \beta(z) \cdot \tau_a^2(z) \cdot z}{(r^2 + z^2)^{1.5}} \cdot r\, dr\, dz. \tag{25}$$

We note that the ratio of the pulse energy to the pulse duration is called peak power. Equation (25) shows that the backscattered power is proportional to the product of the backscatter coefficient and the peak power. Finally, the backscattered pulse radiant exposure

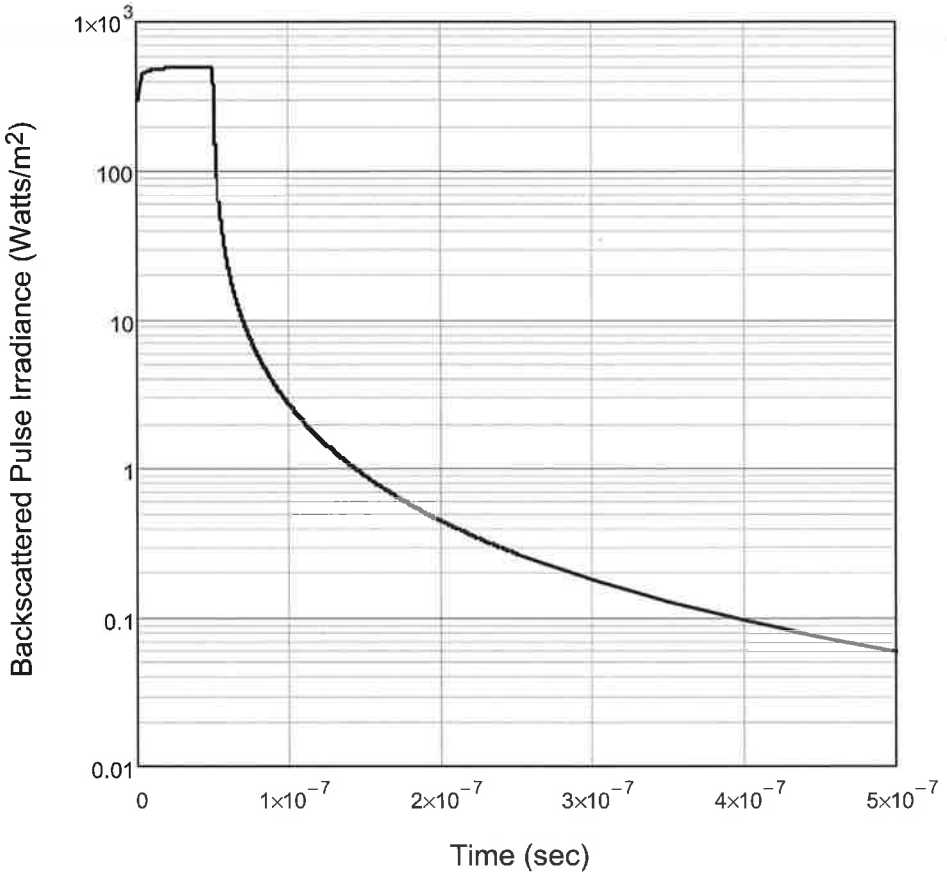

Fig. 2. Typical backscattered irradiance waveform on the aperture plane produced by a propagating laser pulse.

at the origin, $H_{s,P}$, is given by

$$H_{s,P} = \int_0^\infty E_{s,P}(t) \cdot \mathrm{d}t. \tag{26}$$

Figure 2 shows the typical temporal behavior of the backscattered irradiance from a single outgoing pulse as calculated with Eq. (25). For this calculation, we assumed a horizontal propagation path, a laser wavelength of 1.064 μm, a beam radius at the aperture of 0.2 m, a pulse energy and duration of 1 J and 50 ns, respectively, and a beam focus distance of 1 km. The backscatter and extinction coefficients were 2×10^{-6} m$^{-1} \cdot$ sr^{-1} and 9×10^{-6} m^{-1}, respectively. For other input parameter values, the temporal behavior of the backscattered irradiance is qualitatively similar to that shown in Fig. 2.

Figure 2 shows that for times between zero and the pulse duration, the backscattered irradiance rises rapidly from zero to its maximum value. After reaching its maximum, the backscattered irradiance decays, so that after a time of 500 ns its value has been reduced by a factor of 10^{-4} from its maximum value. From Fig. 2 we can see that the backscattered irradiance resembles a pulse waveform. If we define the term pulse width as the time interval

over which a pulse is reduced to half its maximum value, we can see from Fig. 2 that the backscattered pulse duration is slightly longer than the width of the pulse in the beam.

We may therefore conclude that every pulse of a pulsed beam that propagates in the atmosphere will generate a backscattered pulse that propagates back toward the laser source. Therefore, an observer at or near this location will be exposed to a train of backscattered pulses. In Sec. 5, we discuss how the results of this section can be applied to assess the hazard posed by the backscattered pulse train.

4.3. Derivation of the LIDAR equation

LIDAR is a technique in which a pulsed laser is used to make remote, range-resolved measurements of the properties of the atmosphere. In addition to a transmitter that generates the outgoing beam, a LIDAR system employs a receiver that collects the return pulses produced by transmitted pulses that have been backscattered by atmospheric aerosols and molecules. In remote sensing applications, the collected return pulses originate from regions that are at large distances from the system. Equivalently, the time at which the return pulse arrives at the receiver is very much longer than the pulse duration. Under these conditions, the irradiance of the return pulse, $E_{s,L}(t)$, is given by the LIDAR equation

$$E_{s,L}(t) = \beta(R) \cdot Q \cdot \frac{c}{2} \cdot \frac{1}{R^2} \cdot \exp\left[-2 \cdot \int_0^R \mu(z)\,\mathrm{d}z\right], \tag{27}$$

where $R = ct/2$ and $\mu(z)$ is the path-dependent atmospheric extinction coefficient defined in a manner analogous to $\beta(z)$. The last factor on the right side of Eq. (27) is the square of the path-dependent attenuation at $z = R$, $\tau_a^2(R)$. As a check on the validity of Eq. (23), we now show how the LIDAR equation can be derived from Eq. (23) under the appropriate assumptions.

At times t that are much longer than τ, the pulse will have traveled a distance that is very much greater than the characteristic radius of $|\xi(x, y, z)|^2$ in the x–y plane. The quantity $|\xi(x, y, z)|^2$, and hence the integrand in Eq. (23), will be small for x and y outside the region bounded by this radius. Therefore, the sum $x^2 + y^2$ in the denominator will be much smaller than z^2 and Eq. (23) may be approximated by

$$E_{s,P}(t) \cong \frac{Q}{\tau} \cdot \int_{[c(t-\tau)]/2}^{ct/2} \int_{-\infty}^{\infty} \int_{-\infty}^{\infty} \frac{|\xi(x, y, z)|^2 \cdot \beta(z) \cdot \tau_a^2(z)}{z^2}\,\mathrm{d}x\,\mathrm{d}y\,\mathrm{d}z. \tag{28}$$

Using Eq. (10) we can perform the integration over x and y:

$$E_{s,P}(t) \cong \frac{Q}{\tau} \cdot \int_{[c(t-\tau)]/2}^{ct/2} \frac{\beta(z) \cdot \tau_a^2(z)}{z^2}\,\mathrm{d}z. \tag{29}$$

The change in β and τ_a over the limits of integration is negligible, so that both may be taken out of the integral and evaluated at $z = ct/2$. The resulting integral is

$$\int_{[c(t-\tau)]/2}^{ct/2} \frac{\mathrm{d}z}{z^2} = \frac{\tau}{(c/2)t \cdot (t-\tau)}, \tag{30}$$

and because t is assumed to be much greater than τ, we may approximate the right-hand side by $\tau/(c/2) \cdot t^2$. Substituting these results in Eq. (29), we find that

$$E_{s,P}(t) = \beta(ct/2) \cdot Q \cdot \frac{c}{2} \cdot \frac{1}{(ct/2)^2} \cdot \exp\left[-2 \cdot \int_0^{ct/2} \mu(z) \cdot \mathrm{d}z\right], \tag{31}$$

which is Eq. (27). Thus, we have shown that the widely used LIDAR equation may be derived from Eq. (23) under assumptions that are valid for remote sensing scenarios.

5. Application to Backscatter Hazard Assessment

The procedures for assessing the direct beam hazard posed by CW and pulsed laser beams are documented in the ANSI Z136.1-2007 standard.[1] In this section, we discuss how the results derived earlier in this paper may be used to calculate the parameters required by these procedures in order to evaluate backscatter hazards from CW and pulsed beams.

5.1. CW laser

The time-independent backscattered irradiance produced by a CW beam may be thought of as a CW beam that propagates back toward the x–y plane, potentially creating a direct beam hazard for an observer on the x–y plane. In this discussion we will therefore assume that the ANSI methodology for evaluating direct CW beam hazards can be applied to assess potential hazards associated with backscatter from a CW beam.

For a CW laser, the maximum permissible exposure (MPE) is found from the laser wavelength and the total exposure duration. In addition to the MPE, the procedure specified in the ANSI standard also requires the limiting aperture diameter D_f, which for some laser wavelengths depends on the exposure time. The appropriate limiting aperture diameter for the wavelength and exposure time of interest may be found in Table 8 of the ANSI standard. For example, for the spectral range of 0.4–1.4 μm and for exposure durations between 10^{-13} and 3×10^4 s, the limiting aperture diameter for the eye is 7.0 mm. The limiting aperture diameter is subsequently used to calculate the effective power, which is defined to be the power transmitted through an aperture with diameter D_f. For a Gaussian beam profile, the effective power is calculated from a closed-form expression that depends on D_f and the beam diameter.

An analogous closed-form expression does not exist for calculating the effective power from the backscattered irradiance. To derive the effective power, we must first determine the backscattered irradiance at arbitrary locations on the x–y plane. This is accomplished by exploiting the rotational symmetry of our beam model about the z axis. This symmetry implies that the backscattered irradiance will be constant on any circle in the x–y plane whose center coincides with the origin of the coordinate system shown in Fig. 1. In other words, the backscattered irradiance will vary only with distance from the origin and will be independent of the azimuth angle about the origin. It follows that the variation of the irradiance with distance from the origin will be the same on any line that starts at the origin. If we select the y axis as this line, the expression for the backscattered irradiance as a function of distance from the origin, ρ, is given by

$$\tilde{E}_{s,\mathrm{CW}}(\rho) = \Phi \cdot \int_0^{+\infty} \int_0^{+\infty} \int_0^{2\pi} \frac{|\zeta(r,z)|^2 \cdot \beta(z) \cdot \tau_a^2(z) \cdot z}{[(r \cdot \cos\varphi)^2 + (r \cdot \sin\varphi - \rho)^2 + z^2]^{1.5}} \cdot r \cdot \mathrm{d}\varphi \, \mathrm{d}r \, \mathrm{d}z. \tag{32}$$

We should note that a plot of $\tilde{E}_{s,\mathrm{CW}}$ as a function of ρ, which can be generated using Eq. (32), reveals the spatial properties of the backscattered irradiance on the x–y plane. In particular, we may use this plot to visually inspect the value, width, and location of the maximum backscattered irradiance on the x–y plane. A representative plot of the backscattered irradiance on the aperture plane as a function of distance from the aperture

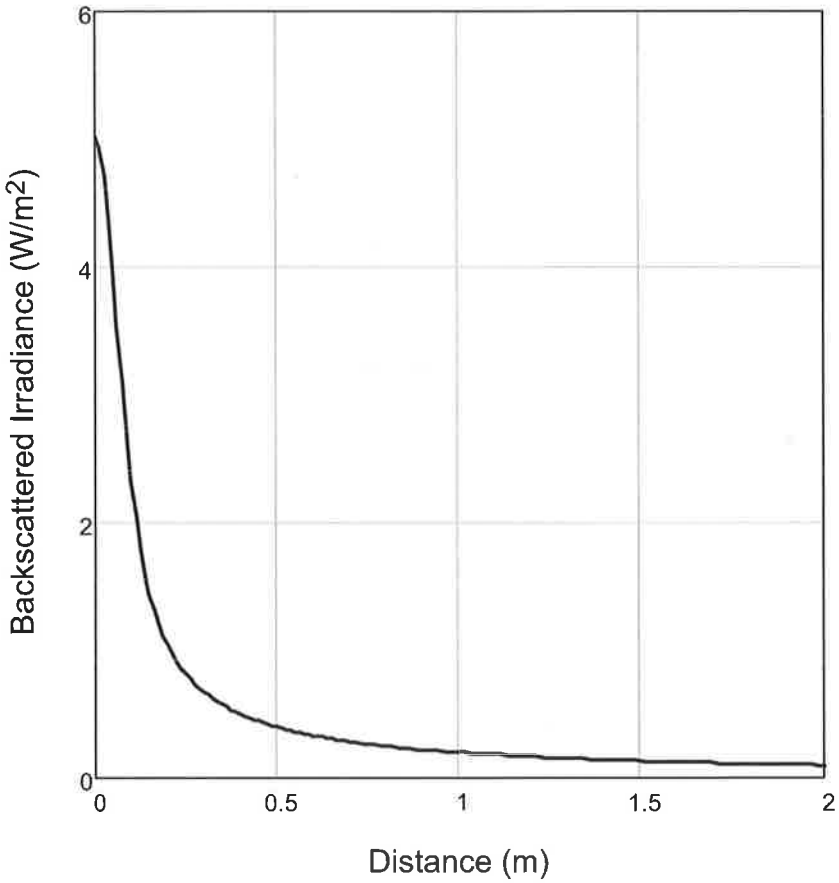

Fig. 3. Example backscattered irradiance on the aperture plane as a function of distance from the aperture center.

center generated using Eq. (32) is shown in Fig. 3. For this calculation, the laser wavelength was 1.064 μm, the beam radius at the aperture was 0.1 m, the beam power was 10^5 W, and the beam focus distance was 1 km. The backscatter and extinction coefficients were 2×10^{-6} m^{-1} sr^{-1} and 9×10^{-6} m^{-1}, respectively.

As shown in Fig. 3, for our beam irradiance model using Eqs. (12) and (13) the maximum irradiance occurs at the aperture center. If the maximum backscattered irradiance occurs at the aperture center, the effective power $\Phi_{S,\mathrm{CW}}$ is found by integrating $\tilde{E}_{s,\mathrm{CW}}(\rho)$ over a circular area of diameter D_f centered at the origin:

$$\Phi_{s,\,\mathrm{CW}} = 2 \cdot \pi \cdot \int_0^{D_f/2} \tilde{E}_{s,\mathrm{CW}}(\rho) \cdot \rho \, \mathrm{d}\rho. \tag{33}$$

A hazardous condition exists when the ratio of the effective power to the product of the MPE and the area of the limiting aperture is greater than unity. In the event that Eq. (32) has its maximum at a point on the aperture plane other than the center, then the effective power must be calculated by integrating $\tilde{E}_{s,\,\mathrm{CW}}(\rho)$ over a circular region of diameter D_f centered at the point of maximum irradiance.

If a hazardous condition exists on the aperture plane, it is sometimes useful to know the distance from the point of maximum irradiance to a location at which the irradiance has decreased to a nonhazardous level. To find this distance, the calculation of the effective power for different circular regions, each with diameter D_f but centered at different distances from the location of maximum irradiance, must be repeated. The effective power calculated in each case will decrease with increasing distance from the location of maximum irradiance. The distance beyond which a hazard does not exist will be that for which the corresponding effective power is equal to the product of the MPE and the area of the limiting aperture.

Note that if the change in $\tilde{E}_{s,\mathrm{CW}}(\rho)$ between $\rho = 0$ and $\rho = 0.5D_f$ is small, the effective power given by Eq. (33) can be approximated by the product of the limiting aperture area and the maximum backscattered irradiance, $\tilde{E}_{s,\mathrm{CW}}(0)$. Therefore, when this approximation is valid, the ratio of the effective power to the product of the MPE and the limiting aperture area, which is used to test for the existence of a hazardous condition, is given by the ratio of the maximum backscattered irradiance to the MPE.

5.2. Pulsed beam

Based on the discussion of Sec. 4.2, each pulse that propagates in the atmosphere will produce a backscattered pulse that propagates toward the location of the laser source. Therefore, an observer at or near this location will be exposed to a train of backscattered pulses. The backscattered pulse train is analogous to that produced by a repetitively pulsed laser. In this discussion we will therefore assume that the ANSI methodology for assessing direct beam ocular and skin hazards from repetitively pulsed lasers can be applied to assess the hazards posed by the backscattered pulse train. A concise tutorial on the application of the ANSI procedures for pulsed beam hazard assessment is given in Ref. 8.

The MPE for a pulsed beam is found from the laser wavelength, the pulse repetition frequency (PRF), the pulse duration, the pulse energy, and the exposure duration. The laser wavelength and PRF of the backscattered pulse train are assumed to be equal to the wavelength and PRF of the outgoing pulse train. The term "pulse duration" is defined in the ANSI standard as the time interval between the half-power points on the leading and trailing edges on the pulse. To find the width of the backscattered pulse, one uses Eq. (25) to plot the backscattered pulse irradiance at the center of the aperture as a function of time as in Fig. 2. The pulse width is estimated from this plot as the time at which the pulse irradiance is reduced to half its maximum value.

The pulsed beam hazard assessment procedure also uses the limiting aperture diameter, but instead of the effective power it uses the effective pulse energy, which is defined to be the pulse energy transmitted through an aperture with diameter D_f. Exploiting the rotational symmetry of the beam model as in the derivation of Eq. (32), we again find that the backscattered irradiance from a single laser pulse depends only on the distance from the origin. Using steps similar to those that led to Eq. (32), we find that the backscattered irradiance as a function of distance from the origin, ρ, and time, t, is given by

$$\tilde{E}_{s,P}(\rho, t) = \frac{Q}{\tau} \cdot \int_a^{ct/2} \int_0^{+\infty} \int_0^{2\pi} \frac{|\zeta(r, z)|^2 \cdot \beta(z) \cdot \tau_a^2(z) \cdot z}{[r \cdot \cos\varphi^2 + (r \cdot \sin\varphi - \rho)^2 + z^2]^{1.5}} \cdot r \cdot \mathrm{d}\varphi \, \mathrm{d}r \, \mathrm{d}z. \tag{34}$$

A plot of $\tilde{E}_{s,P}$ as a function of ρ for a fixed t, e.g., at $t = \tau$, generated using Eq. (34) reveals the spatial properties of the backscattered irradiance on the x–y plane. In particular,

this plot can be used to visually inspect the value, width, and location of the maximum backscattered irradiance on the x–y plane. If the maximum backscattered irradiance occurs at the aperture center, the backscattered pulse power passing through the limiting aperture at time t, $\Phi_{S,P}(t)$, is found by integrating $\tilde{E}_{s,P}(\rho, t)$ over a circular area of diameter D_f centered at the origin:

$$\Phi_{s,P}(t) = 2 \cdot \pi \int_0^{D_f/2} \tilde{E}_{s,P}(\rho, t) \cdot \rho \, \mathrm{d}\rho. \tag{35}$$

The effective energy is then found by integrating $\Phi_{s,P}(t)$:

$$Q_{s,P} = \int_0^{\infty} \Phi_{s,P}(t) \, \mathrm{d}t. \tag{36}$$

A hazardous condition exists when the ratio of the effective energy to the product of the single-pulse MPE and the area of the limiting aperture is greater than unity. In the event that Eq. (34) has its maximum at a point on the aperture plane other than the center, then the backscattered pulse power must be calculated by integrating $\tilde{E}_{s,P}(\rho, t)$ over a circular region of diameter D_f centered at the point of maximum irradiance. We note that the total energy in the backscattered pulse may be calculated by letting the upper limit of the integral in Eq. (35) go to infinity and substituting the resulting function of time in the integral on the right side of Eq. (36).

Further, we note that if the change in $\tilde{E}_{s,P}(\rho, t)$ between $\rho = 0$ and $\rho = 0.5\ D_f$ is small, the backscattered pulse power given by Eq. (35) can be approximated by the product of the limiting aperture area and the maximum backscattered irradiance, $\tilde{E}_{s,P}(0, t)$. If we substitute this product for $\Phi_{s,P}(t)$ in Eq. (36), we find that

$$Q_{s,P} \cong \frac{\pi \cdot {D_f}^2}{4} \cdot \int_0^{\infty} \tilde{E}_{s,P}(0, t) \, \mathrm{d}t. \tag{37}$$

The integral in Eq. (37) is the maximum backscattered radiant exposure and is calculated numerically using Eq. (25). Therefore, when this approximation is valid, the ratio of the effective energy to the product of the MPE and the area of the limiting aperture, which is used to test for the existence of a hazardous condition, is given by the ratio of the maximum backscattered radiant exposure to the MPE

6. Conclusions

High-energy lasers propagating in the atmosphere will generate backscattered radiation that may create ocular and skin hazards to personnel at the location of the laser source. The equations that quantify the backscattered irradiance from both CW and pulsed lasers were derived based on the definition of the backscatter coefficient and beam propagation theory. The approximate results derived in this paper are appropriate for determining whether hazardous conditions exist for personnel in the vicinity of the laser source. Our analysis has shown that the backscattered irradiance is a function of the laser power and the atmospheric backscatter coefficient along the propagation path. The latter depends on the aerosol concentrations and the atmospheric conditions present at the test or deployment location. Therefore, in order to assess the hazard from exposure to backscattered radiation in a specific high-energy-laser test or deployment scenario, one needs to know, or at least be able to estimate an upper bound for, the backscatter coefficient at the laser wavelength and the test or deployment location.

References

[1]American National Standards Institute, *American National Standard for Safe Use of Lasers, ANSI Z136.1-2007*, Laser Institute of America, Orlando, FL (2007).

[2]Born, M., and E. Wolf, *Principles of Optics*, 6th ed., pp. 633–656, Pergamon Press, Oxford, UK (1980).

[3]Hinkley, E.D. (Ed.), *Laser Monitoring of the Atmosphere*, Springer, Berlin (1976).

[4]Measures, R.M., *Laser Remote Sensing: Fundamentals and Applications*, Wiley, New York (1984).

[5]Schott, J.R., *Remote Sensing*, pp. 80–82, Oxford University Press, New York (1997).

[6]Shette, E.P., and R.W. Fenn, "Models of the Aerosols of the Lower Atmosphere and the Effects of Humidity Variations on Their Optical Properties," AFGL-TR-79-0214, Environmental Research Papers No. 676, Air Force Geophysics Laboratory, Hansom Air Force Base (1979).

[7]Smullin, L.D., and G. Fiocco, Nature **199**, 1275 (1963).

[8]Thomas, R.J., B.A. Rockwell, W.J. Marshall, R.C. Aldrich, S.A. Zimmermann, and R.J. Rockwell, J. Laser Appl. **13**, 134 (2001).

The Authors

Dr. Edward Early received a B.S. degree in physics from Texas A&M University in 1984 and M.S. and Ph.D. degrees in physics from the University of California, San Diego, in 1987 and 1991, respectively. Following a postdoctoral position in high-temperature superconductor research, he joined the Optical Technology Division of the National Institute of Standards and Technology, where he worked on standards and calibrations for spectrophotometry, color and appearance, and remote sensing. He joined TASC in 2004 and currently supports the Optical Radiation Branch of the Air Force Research Laboratory in the area of high-energy laser safety analyses, specifically developing analysis techniques and researching reflecting properties of materials at high temperatures. He is a member of DEPS, OSA, and ANSI.

Dr. Paul Kennedy received B.S., M.S., and Ph.D. degrees in physics from North Texas State University in 1976, 1980, and 1983, respectively. In 1983 he joined the Rocketdyne Division of Rockwell International, where he served as a theoretical analyst and scientific programmer supporting research and development on high-energy lasers. Since 1992 he has been a Senior Research Biophysicist in the Optical Radiation Branch of the Air Force Research Laboratory, characterizing and modeling the interaction of lasers and other optical radiation with biological systems, primarily the eyes and skin. In this capacity he has developed theoretical models and performed numerous analytical studies to predict laser-induced tissue damage and its effect on military operations. He is currently a senior scientist and technical advisor to the USAF High Energy Laser Safety Program. He is a member of APS, OSA, DEPS, and SPIE

Dr. George Megaloudis received B.A. and Ph.D. degrees in physics from Northeastern University in 1970 and 1977, respectively. Since 1981 he has been with TASC, where he has performed technical analyses and prototype system design in a broad range of technologies. These include remote sensing, RF and electro-optical active and passive sensors, signal processing, statistical analysis, pattern recognition, numerical simulation, and atmospheric phenomenology. Currently, he performs laser safety analyses to support high-energy-laser field tests. In this capacity, he developed theoretical models and several prototype tools to predict the properties of high-energy-laser radiation reflected from real-world targets.